Morphology and Transport in Eukaryotic Cells

Anamika Agrawal,[1] Zubenelgenubi C. Scott,[1] and Elena F. Koslover[1]

[1] Department of Physics, University of California, San Diego, San Diego, CA 92093, USA; email: ekoslover@ucsd.edu

Xxxx. Xxx. Xxx. Xxx. YYYY. AA:1–21

https://doi.org/10.1146/((please add article doi))

Keywords

intracellular transport, organelles, cytoskeleton, networks, cell morphology

Abstract

Transport of intracellular components relies on a variety of active and passive mechanisms, ranging from the diffusive spreading of small molecules over short distances, to motor-driven motion across long lengths. The cell-scale behavior of these mechanisms is fundamentally dependent on the morphology of the underlying cellular structures. Diffusion-limited reaction times can be qualitatively altered by the presence of occluding barriers or by confinement in complex architectures, such as those of reticulated organelles. Motor-driven transport is modulated by the architecture of cytoskeletal filaments that serve as transport highways. In this review we discuss the impact of geometry on intracellular transport processes that fulfill a broad range of functional objectives, including delivery, distribution, and sorting of cellular components. By unraveling the interplay between morphology and transport efficiency, we aim to elucidate key structure-function relationships that govern the architecture of transport systems at the cellular scale.

Contents

1. Introduction

Eukaryotic cells face the dual task of maintaining a complex spatial organization, including sorting and sequestration into different subcellular structures, while at the same time being able to transport components efficiently within and among those structures. Unraveling the coupling between subcellular morphology and the dynamics of transport is critical to understanding structure-function relationships at the cellular scale.

The general mechanisms involved in intracellular transport have been extensively characterized, both for *in vitro* reconstituted systems and in live cells. Small molecules moving over short distances can rely on diffusion-like transport driven by broadly dispersed fluctuations in the intracellular medium (33, 40, 53). Proteins, for example, have a cytoplasmic diffusivity on the order of $10\mu m^2/s$, and metabolites diffuse an order of magnitude faster still (85). Larger particles, such as vesicles ($\sim$ 100nm) and RNA molecules ($\sim$ 40nm), or extended cell regions, such as neuronal projections (100μm - 1m), fungal hyphae ($10-100\mu$m), and large oocytes (100μm-1mm), require active motor-driven transport along cytoskeletal highways (at speeds of $0.1 - 2\mu$m/s) for efficient distribution across the cell (85). In addition to being able to traverse long distances, motor-driven motion allows for a plethora of regulatory mechanisms that control delivery and sorting of cargo among specific cellular regions (24, 46, 62). In certain cell types, ranging from slime molds (5) to algal cells (50) to fly oocytes (97), long-range fluid flows in the cytoplasm (at speeds of $0.3 - 1000\mu$m/s) also contribute to the delivery and distribution of particles.

Intracellular morphology plays a critical role in determining the efficiency of each of these transport mechanisms, as well as the balance between their contributions. Active motion (through motors or flows) becomes increasingly important as the path length between the particle starting point and its target increases (88). This path length can be extended by the formation of long cellular projections, as in neurites, or by the presence of barriers that hinder diffusive passage. At the same time, the spatial architecture of cytoskeletal filaments governs the long-range behavior of motor-driven cargos, allowing for efficient sorting between subcellular destinations (46, 62, 124), for faster target search times (54, 112), and for enhanced precision of cargo localization in space and time (49).

The physical and molecular mechanisms underlying diffusive transport (21, 33, 75), motor-driven motion (11, 46, 55), and cytoplasmic streaming (50, 97), as well as their effective behavior on a cellular scale (24, 88), have been extensively reviewed elsewhere. In this review, we focus on the interplay of spatial architecture and transport dynamics in

the context of different cellular transport systems. In Section 2, we consider the effect of structural features such as tubular networks and occluding barriers on the diffusive distribution of molecules through the cell. In Section 3, we turn to motor-driven transport and explore the role of cytoskeletal organization in a variety of cellular transport systems. We end with a brief overview of important questions and future challenges in this field. Rather than attempting an exhaustive coverage of morphology-transport coupling, we aim to delineate key general principles for how intracellular architecture regulates, limits, and enhances transport processes, highlighting illustrative examples as we go.

2. Intracellular morphology and diffusive transport

Most biomolecular pathways rely on the diffusive encounter of molecules within a cellular fluid or lipid membrane environment. Many such pathways are embedded within domains of complex geometry, determined by the morphology of either the cell itself or of intracellular organelle structures. Here we review some key conceptual results regarding the impact of domain morphology on diffusive search.

2.1. Diffusion on a fractal

One fruitful approach to modeling diffusion in a complex geometry treats both the particle dynamics and the geometry as continuous, scale-free fractals. Such a model assumes that zooming in to ever-smaller length scales does not change the system, implying that pores and obstacles, as well as step sizes, exhibit a broad power-law distribution over many scales (16). Fractal structures have been used to describe biological morphologies ranging from neuronal trees (14) to the cortical actin meshwork (102), to mitochondrial networks and the cytoplasm itself, within certain length limits (8, 15).

In this framework, search times are dictated by two fractal dimensions. The dimension d_w of a random walk is defined by the scaling of its mean squared displacement: MSD $\sim t^{2/d_w}$ (16), or equivalently the scaling for the time to exit a sphere of radius R: $t_{\text{exit}} \sim R^{d_w}$ (30). Classic Brownian diffusion has a dimension of $d_w = 2$, with higher dimensionality for subdiffusive fractional Brownian motion (such as observed in a viscoelastic continuum (65)), and lower dimensionality for Lévy flights (arising from active processive motion (26) or exploration of a folded filament by hopping in three-dimensional space (31)). The dimension of a domain relates its volume (or the number of sites, N, in a discrete lattice model) to its spatial extent (R) according to $N \sim R^{d_f}$. An unobstructed three-dimensional domain has $d_f = 3$, confinement to a membrane or narrow tubule can give effective dimensionality $d_f = 2$ or $d_f = 1$, respectively. More complex morphologies, such those of a cytoplasm or membrane region crowded with obstructions across many size scales (8, 15, 102), can have a fractional dimension d_f (Fig. 1a).

Target search processes on a fractal domain fall into two general classes (16, 17). Compact search occurs in the regime with $d_w > d_f$ and corresponds to a particle that thoroughly covers each region of the domain it visits, leaving no gaps behind (Fig. 1a.iv). In this regime, search times are strongly dependent on the distance between the particle source and the target, and a particle starting near its target is very likely to find it without ever reaching the domain boundary. For a compact search process, the search rate scales super-linearly with the target concentration (mean search time $\sim N^{d_w/d_f}$) and the search times exhibit a broad long-tailed distribution that is not well represented by the mean time (17).

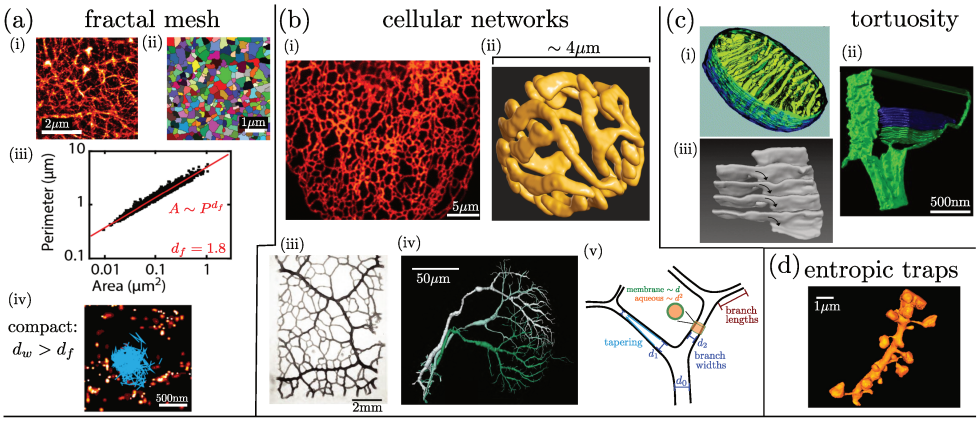

Figure 1

Morphological features of cellular structures modulate diffusive transport. (a) (i) Fractal architecture of cortical actin obtained with super-resolution imaging; (ii) compartments formed by filaments exhibit (iii) fractal morphology of dimension $d_f = 1.8$. (iv) Trajectory of plasma membrane channel shows compartmentalization resulting in compact exploration dynamics. Figure adapted from Reference (102), CC BY. (b) Example cellular network structures include (i) peripheral endoplasmic reticulum in a mammalian cell (data provided by Laura Westrate), (ii) yeast mitochondrial network (image provided by Matheus Viana), (iii) slime mold *P. polycephalum* plasmodium (adapted with permission [pending] from Reference (4)), (iv) dendritic trees of *Drosophila* optical sensory neurons (adapted from Reference (19), CC BY); (v) schematic of key parameters that govern particle transport through a dendritic tree. (c) Example intracellular structures that increase tortuosity for diffusing particles; (i) mitochondrial cristae (adapted with permission from Reference (42)), (ii) membranous discs in outer segment of rod photoreceptor (adapted with permission from Reference (132)), (iii) ER perinuclear sheet stack connected by spiral dislocation (adapted with permission from Reference (126)). (d) Dendritic spines serve as entropic traps for diffusing particles (image from mouse pyramidal neurons; adapted from Reference (127), CC BY).

By contrast, non-compact search ($d_w < d_f$) involves sparse sampling of subregions, so that most particles explore the full extent of the domain before ever encountering the target. This is the regime of mass action kinetics, with search rates proportional to concentration (mean search time $\sim N$). Notably, switching from bulk to compact kinetics (*eg:* by confinement to a membrane surface) increases the frequency of rebinding events and can convert a distributive enzymatic process into a processive one, wherein the substrate remains effectively associated with a single enzyme for multiple sequential reactions (123). This switch can have profound functional consequences, including the suppression of bistability and ultrasensitivity in a multi-step reaction pathway (1, 123).

2.2. Diffusion on networks

An alternate perspective on diffusion in complex geometry treats the domain structure as a network of interconnected tubes and containers. The architecture of such networks modulates both the overall spreading of particles (74) and the kinetics of encounter with reactive targets (23, 71, 75). Network structures (Fig. 1b) can be used to describe polymorphic organelles such as the peripheral endoplasmic reticulum (23, 44) and mitochondria (131, 140),

as well as cellular-scale morphologies in a variety of cell types, including branched neuronal axons or dendrites (41, 60, 106), slime molds (6, 4), and fungal mycelia (43).

2.2.1. Modeling random walks on networks. Random walks on network structures have been studied extensively for applications ranging from porous media to urban transportation (see (81) for a review). For a given distribution of transition times between connected nodes, the low-order moments of the first passage times between any two nodes on the network can be calculated directly (51, 114). Analysis of mean first passage times on varying network structures leads to a number of general results. One is that the accessibility of different regions in a network can be highly heterogeneous, with several 'centrality' metrics developed to quantify the importance of a node in network search processes (13, 93). Another is the asymmetry of search on a network: the mean first passage time from one node to another can be orders of magnitude greater than the mean first passage time for the reverse transition (93).

Cellular transport relies on a specific class of network structures termed geographic or spatial networks. These networks are characterized by nodes with a well-defined location in space, and a distance-dependent connectivity where each node is most likely to be connected to its nearest spatial neighbors (13). The efficiency of particle distribution through a spatial network is highly dependent on the node layout and connectivity, with optimal architectures explored in the context of public transportation (47), flow-driven nutrient delivery in slime molds (80, 83), vasculature systems (101), and organelle morphologies (23, 131).

Diffusive propagation in a spatial network is limited by the lengths of connecting tubules (114) and by the escape time from compartments at individual nodes (71, 74). The latter can be modeled as a narrow escape problem from a small hole of size ϵ on the boundary of a cavity of size R, with escape times scaling as $R^3/(D\epsilon)$ in a 3D compartment and $\left(R^2/D\right)\log(R/\epsilon)$ in a 2D one (18, 110). When these escape times are relatively slow, particles exhibit a compact search process, thoroughly exploring each compartment before hopping to the next (71). Such behavior has been observed for the motion of membrane proteins corralled by the cortical actin meshwork (Fig. 1a.iv) (102) and for cytoplasmic proteins compartmentalized by the tubules of the endoplasmic reticulum (69).

2.2.2. Cellular networks: tubular and tree structures. One important class of cellular networks is composed of percolating structures of interconnected tubules. Tubular network architectures are observed for two critical eukaryotic organelles – the endoplasmic reticulum (ER)(23, 44, 135) and fused mitochondria networks (131, 140) (Fig. 1b). These networks host a number of functionally important biomolecular reaction pathways, including the protein quality control pathways within the ER and the binding of regulatory factors to nucleoids within mitochondria. The proteins involved in these pathways rely largely on diffusion to find each other and carry out their functions. Furthermore, both organelles play a critical role in calcium homeostasis within the cell, with localized release of ER calcium requiring intra-organelle transport from other regions of the network (66).

Peripheral ER and mitochondrial networks have relatively small junction regions, so that movement across the network is dominated by the timescale of passing along each tubule and by the tubule connectivity. Such networks can be treated as percolation lattice systems – a generalized model for structures with evenly distributed nodes and some amount of missing connectivity between neighbors (8, 23, 122). When the neighbor connection probability approaches close to a critical value, percolation systems exhibit universal power-

law scaling behaviors for transport quantities such as the effective diffusivity and search times of particles on the network (16, 120).

Both the peripheral ER in adherent mammalian cells (23, 73) and the surface-confined mitochondrial networks of yeast cells (131) form nearly planar structures with evenly distributed nodes. Averaged search times on such networks tend to be dominated by two global parameters: the total edge length and the network loop number. Networks with low total edge length and high connectivity result in the fastest search kinetics, and the scaling of search times with these two global parameters can be predicted by mapping to a percolation system (23). Deletion of the proteins responsible for mitochondrial fusion and fission results in yeast mitochondrial networks with reduced looping connectivity, and simulations indicate that this morphological change may substantially lower kinetic rates for particles at low copy number (131).

In some cellular tubule networks, diffusive transport is greatly accelerated by the presence of flows that arise from tubule contraction. One well-studied example are the peristaltic waves of contraction that help deliver material throughout the plasmodium network of the slime mold *Physarum polycephalum* (5, 4) (Fig. 1b.iii). Such waves enhance diffusive mixing via Taylor dispersion (9), with the effective dispersion coefficient increased by pruning of the network architecture into a hierarchy of tubules of varying thickness (80). On a smaller scale, luminal proteins in the peripheral ER network exhibit short processive motions that have been hypothesized to arise from uncoordinated tubule contractions (58). These flows may lead to transport of particles in discrete packets, with the most rapid mixing observed for intermediate values of the flow persistence time (35).

Another important class of cellular networks are the branching, loop-less trees that describe the morphology of neuronal projections (Fig. 1b.iv). Dendritic trees exhibit hierarchically branched structures, with heterogeneous branch widths that taper away with distance from the soma (38, 72). While active motor-driven transport plays an important role in distributing components throughout the dendritic tree, passive diffusion remains critical for the local dispersion and distribution of distally translated proteins (41).

The architecture of the branched network, including branch lengths, widths, and tapering (Fig. 1b.v), determines the concentration gradients established by diffusive molecules produced at either the soma or the distal tips. Neuronal pathologies associated with aging and Alzheimer's disease are known to reduce the depth of the dendritic tree, potentially interfering with the formation of such gradients (60). The narrowing of dendritic branches along the tree implies an increased surface-area-to-volume ratio, resulting in enhanced diffusive transport of membrane versus luminal proteins towards the distal tips (106). This observation highlights the inherent directional biases that arise for diffusive transport in tubules of varying cross-sectional area (142). Interestingly, the observed statistics of branch thickness in pyramidal neuron dendrites imply that they may be tuned to optimally and evenly distribute a variety of neuronal proteins (106), suggesting diffusive protein transport as one of the functional objectives modulated by dendritic morphology (72).

2.3. Tortuosity and traps

Another role for geometry in modulating transport is the curtailing of particle diffusion by local traps and occluding barriers. Subcellular structures can form physical barriers that force individual particles to follow highly convoluted paths to reach from the source site to the target. This effect is measured by the 'tortuosity' of the domain, defined as the ratio

between the typical length traversed by a diffusing particle and the straight-line distance between start and end points (115). A tortuosity of τ can be used to scale the diffusion coefficient according to $D_{\text{eff}} = D/\tau^2$ when describing diffusion through porous or crowded media(67, 115).

Cellular obstacles, like folded cristae in mitochondria (Fig. 1c.i) and membranous disc stacks in the outer segment of photoreceptor cells (Fig. 1c.ii), can increase local tortuosity and thereby slow axial diffusivity (up to 5-fold inside mitochondria (32) and 20-fold in photoreceptors (25)). In the cytoplasm, a broad range of obstacles and compartment sizes give rise to heterogeneous local diffusion and limited long-range spreading of particles (15, 69). Such heterogeneous diffusivity has been proposed to account for the anomalous non-Gaussian distribution of step sizes observed for cytoplasmic particles (29, 68, 133). Notably, closely spaced structures can impose different degrees of volume exclusion and tortuosity on proteins of variable size, yielding steep decreases in diffusivity for larger protein complexes (91). Similar size-dependent effects have been observed in cytoplasmic diffusivity measurements (15, 33).

A unique example of intracellular morphology that must be traversed with highly tortuous paths is provided by the stacks of membranous sheets in the perinuclear endoplasmic reticulum (126). These sheets are interconnected by spiral dislocations that locally resemble a helicoidal 'parking-garage' structure (Fig. 1d.iii). Such connectivity allows membrane or luminal proteins inside the sheet to pass from one layer to another by winding around the spiral dislocations, without needing to find specific narrow connections points, allowing relatively efficient diffusive transport through the stack (59).

Beyond occluding barriers, cellular morphology can slow diffusion by providing localized entropic traps, in the form of locally expanded regions from which the particle must escape before continuing its spread (21, 142). An extreme form of trapping arises from narrow-necked projections branching off a primary path. This morphology is exemplified by dendritic spines, which form mushroom-shaped outgrowths spaced along the dendrite (Fig. 1d). These traps give rise to anomalous subdiffusive motion along the dendritic axis over short timescales, and a reduced effective diffusivity at long times (105). Coarse-grained models of dendritic networks imply that the presence of spines slows mean first passage times of diffusing signaling components from distal tips to the soma by up to 50% (60). Interestingly, neuronal pathologies such as schizophrenia and Down's syndrome may reduce spine volume, while aging and Alzheimer's disease are associated with lowered spine density. Both effects are expected to hinder concentration gradient formation by decreasing trapping in the spines (60).

3. Cytoskeletal architecture and motor-driven transport

For large cargos and long cellular distances, intracellular transport is dominated by active rather than diffusive motion (88). A ubiquitous form of active transport in eukaryotic cells relies on attaching cargo to molecular motors that walk processively along cytoskeletal filaments. The distribution and delivery of motor-driven cargo is modulated by a panoply of molecular factors that regulate motor-cargo and motor-track attachment (45, 113). Transport organization is also heavily dependent on the morphology of the cytoskeletal track arrangement, often closely coupled to the morphology of the cell itself (24, 103). Here we focus on animal and fungal cells, which rely largely on microtubules for long-range transport, with some contribution from actin filaments for local positioning (62) and dispersion (54).

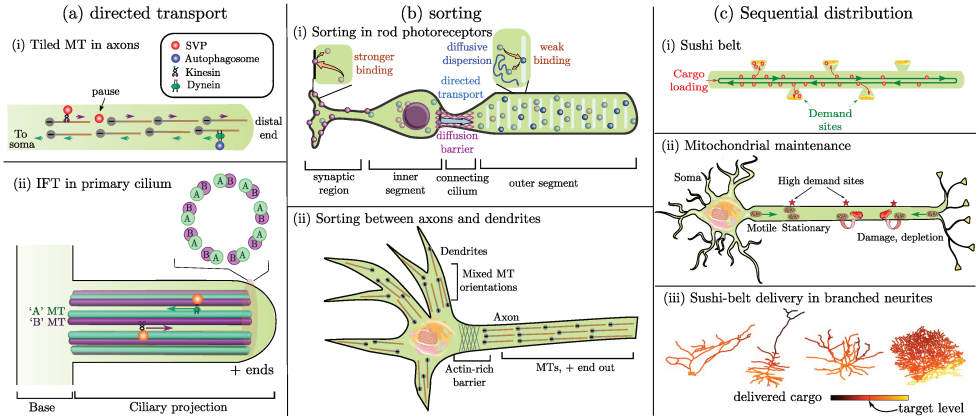

Figure 2

Transport objectives for parallel microtubule architectures in narrow cellular morphologies. (a) Directed delivery: (i) Overlapping tiling of polarized microtubules allows efficient long-range anterograde and retrograde transport in neuronal axons, with cargos tending to pause at microtubule plus-ends and minus-ends, respectively (139). (ii) IFT trains in ciliary projections allow directed transport of molecular components between the base and tip, with alternately marked A and B microtubules precluding collisions between oppositely moving cargo. (b) Sorting between different cell regions: (i) Directed motion through a narrow connecting structure, a diffusive barrier, and reversible local binding combine to sort peripheral membrane proteins to specialized regions of photoreceptor cells (adapted from Reference (22), CC BY-SA). (ii) Differing microtubule polarity and an actin-rich filter structure in the proximal axon allow for sorting of dendritic and axonal cargos. (c) Distribution to sequential target regions: (i) The 'sushi-belt' model describes circulating cargo locally halted at target regions such as dendritic spines or axonal presynaptic boutons (36). (ii) Maintenance of mitochondria stationed at peripheral sites of high energetic demand requires occasional exchange between motile and stationary populations (adapted from Reference (2), CC BY). (iii) Distribution of delivered cargo in different dendritic tree morphologies highlights the reduced accuracy of a sushi-belt delivery system in long or highly branched structures. (image adapted from Reference (136), CC BY).

3.1. Parallel microtubule structures

Parallel arrangements of microtubules are found in narrow cellular projections and in epithelial cells exhibiting planar cell polarity (24). Parallel arrangements can support directed anterograde or retrograde transport between perinuclear regions and the periphery (62, 78), as well as broad dispersion and servicing of multiple consecutive target sites (36, 136, 137). In this section, we explore how structural features of parallel microtubule arrays contribute to a variety of cellular transport objectives.

3.1.1. Directed delivery. A number of narrow cellular projections feature fully polarized arrays of microtubules, with plus-ends pointing towards the distal tip. Examples include the distal regions of fungal hyphae (104), cilia and flagella (121), and neuronal axons (63, 139). These polarized arrangements allow directed delivery of cargos that are carried towards the projection tip by the kinesin family of motors (57) or back towards the soma by dynein motors (100). Examples include anterograde motion of synaptic vesicle precursors (SVPs) and retrograde delivery of mature autophagosomes in axons (77) (Fig. 2a.i), as well as the intraflagellar transport (IFT) trains that deliver components between the base and tip of

primary cilia projections (121, 125) (Fig. 2a.ii).

The directed run-length of motor-driven cargo is governed by mechanochemical coupling between multiple motors (55), by interaction with microtubule-associated and cytoplasmic proteins (12, 11, 34), and by the length of the microtubule tracks themselves. Severing and motor-driven sliding of microtubules (63) allows long cellular regions, such as the axon, to be covered by a tiling of relatively short overlapping filaments (Fig. 2a.i). Cargo can move beyond the length of a single filament and bypass obstacles by stepping between parallel microtubules. Efficiency of such sideways transitions is determined in part by the density and distribution of microtubule filaments within the cross-section of the cylindrical projection. For example, pause durations in axonal transport were shown to be shorter in regions with high local density of microtubules (139).

The microtubule density also limits the rate of a particle first initializing active transport. Such initiation requires a diffusing particle to encounter a microtubule within the cylindrical cross-section, at a rate which scales with the number of available filaments (89). Particles that rely on hitchhiking transport (104) must also wait for a passing carrier organelle along a nearby microtubule, so that tethering to the cytoskeletal filament can greatly accelerate transport initiation (89). In some systems, dynein motors are observed to accumulate into 'dynein comets' at the microtubule plus-ends (90, 111). Cellular cargos need to diffusively find these point-like capture regions to initiate retrograde transport. Mathematical modeling indicates this initiation process is optimized when the microtubule plus-ends are scattered over a broad range of axial positions (87, 114).

An important feature of parallel microtubule arrays is their ability to simultaneously host anterograde and retrograde transport. Collisions between cargo walking in opposite directions along the same microtubule can hinder processive motion, triggering pausing events that are resolved by 3D reorientation of the cargo around the microtubule (130). Some cellular structures have evolved specialized regulatory mechanisms to avoid such collisions. In the axoneme of cilia and flagella (Fig. 2a.ii), each doublet of microtubules serves as a pair of directed tracks, marked by post-translational modifications, with anterograde particles moving along B-microtubules and retrograde particles along A-microtubules (121). This arrangement allows cargos to move fully processively, passing each other in both directions without noticeable pausing or side-stepping (121).

3.1.2. Sorting to Cellular Regions. In addition to enabling rapid delivery to and from distal regions, parallel microtubule architectures also facilitate the sorting of cargo to different cellular compartments. Several physical mechanisms are leveraged by cells to achieve the accumulation of particles in one region and depletion in another. Diffusive transport coupled with regional binding or anchoring can yield local enhancement in bound particle concentrations. With this mechanism, however, increasing the steady-state accumulation of particles requires lower unbinding rates, leading to slower mixing (82) and delayed temporal response to changing conditions.

An alternate approach to sorting relies on directed transport towards a cellular region, which results in accumulation even in the absence of local anchoring. In general, particle concentrations will drop exponentially from the region of flow-driven accumulation, according to $c \sim \exp(-\mathrm{Pe} \cdot x/L)$, where L is the length of the domain. The dimensionless quantity Pe is the Péclet number comparing the relative strength of advective and diffusive transport (49, 88).

Accumulation due to directed transport can be combined with localized binding or hin-

dered diffusion through a narrow connecting region to further enhance particle sorting. This combination of mechanisms is thought to be responsible for the localization of peripheral membrane proteins to the outer segment of rod photoreceptor cells (25, 82) (Fig. 2b.i). In the initial segment of neuronal axons, an actin-rich barrier hinders diffusive entry of components into the axon (119). Only cargos that acquire kinesin-1 motors in the pre-axonal exclusion zone are able to make it past this initial segment and into the axon itself (37, 92).

In neuronal cells, microtubule polarity also plays an important role in cargo sorting among neuronal projections. Specifically, axonal microtubules tend to be fully polarized with plus ends pointing towards the distal tips, while mammalian dendrites exhibit a largely unpolarized microtubule arrangement (64, 138) (Fig. 2b.ii). Dynein-driven cargo is then excluded from the axon but is broadly distributed throughout dendritic regions via bidirectional transport on the mixed microtubule arrays (64, 62).

3.1.3. Distribution across sequential targets. An important challenge for transport through long cellular regions is the effective distribution of particles to multiple targets, either lying sequentially along a linear domain or at the tips and junctions of a branched network. To carry out this task, the cell must regulate both transport direction and halting dynamics to ensure that particles are appropriately distributed over widely separated regions. Such targeted distribution is particularly relevant in neuronal projections, whose extended branched structures exhibit spatial heterogeneity in their metabolic and protein homeostasis needs (56, 98). Specific examples include the stationing of mitochondria at dendritic spines or axonal nodes of Ranvier (3, 2, 27, 99), the transport of mRNAs to regions of high synaptic activity (48), and the delivery of synaptic vesicle precursors to *en passant* synapses (52).

Despite the importance of efficient distribution, there is no known global addressing system in neurons that would enable targeted delivery to one versus another synaptic region. Instead, cellular trafficking relies largely on local signals that halt transport in regions with high demand for a particular cargo (36, 136). This mechanism, which has been termed the 'sushi-belt' model (36), relies on cargos circulating throughout the neuronal tree with sporadic capture at *en passant* boutons (137) or other regions that produce a local stopping signal (Fig. 2c.i).

One example of a local-signal-based distribution system is the halting of mitochondrial transport in response to elevated calcium levels (113) or to the downstream products of glucose metabolism (96). Localization by a diffusive signal requires both rapid decay and intermediate concentration levels of the signaling molecule, to enable steep gradient formation without saturating the kinetics of the biomolecular pathway for halting active transport (3). An alternate mechanism for local stopping relies on enhanced dynamics of the microtubule plus-ends in the vicinity of *en passant* presynaptic regions. Weak binding of processive kinesin-3 motors to the GTP-bound caps characteristic of highly dynamic microtubules is thought to result in cargo being dropped off specifically at the presynaptic zones (52).

Regardless of the precise mechanism, the local halting of cargo transport cannot be absolute if the cargos are to be distributed among multiple sequentially located regions rather than accumulating at the first region nearest to the soma. The sushi-belt model (36) (Fig. 2c.i) assumes that cargo circulating from the soma to the distal tip and back again has a finite probability of stopping at each demand site. Measurements in *Drosophila* neurons show that neuropeptide-carying dense core vesicles are indeed broadly distributed among

many synaptic boutons by bidirectional recirculation coupled with inefficient sporadic capture (137).

Such a distribution system faces an inherent trade-off between the rate and precision of cargo positioning (136). Accurate localization requires a high fraction of time spent in the stationary state, with a correspondingly slower rate of distribution. In cases where the cargo is depleted (*e.g.* aging of distal mitochondria (39)), the steady state distribution among many demand sites depends on the balance between depletion and delivery rates (Fig. 2c.ii). Modeling of mitochondrial maintenance in both linear projections and branched trees indicates the existence of an optimum exchange rate and fraction of mitochondria that should be maintained in a stationary state at local demand sites (2). Additionally, simulations of the sushi-belt model in explicit morphologies for different neuronal cell types indicate that both the precision and distribution rate are lower in long or densely branched neuronal morphologies (136) (Fig. 2c.iii).

3.2. Cytoskeletal network architecture

In many animal cell types, motor-driven cargo transport relies on a centrally nucleated, entangled three-dimensional network of microtubules, aided by a mesh of short actin filaments concentrated at the peripheral cell cortex. The spatial organization of these filaments, including the distribution of intersections and orientations, modulates the ability of cargos to traverse and find targets throughout the cytoplasm.

3.2.1. Cytoskeletal architecture: density and polarity. Several computational (7, 86, 107, 118) and experimental (10, 20, 76, 108) studies have focused on how the explicit spatial distribution of filaments in a bulk cytoskeletal network affects cargo transport. Both *in vitro* and *in vivo* measurements show that microtubule intersections (Fig. 3a) play an important role in limiting cargo processive run-length, with pausing duration and direction of motion after an intersection governed by both the motor complement and the geometry of the intersection itself (10, 130).

A common metric for overall transport efficiency is the mean first passage time (MFPT) for cargo to traverse the cell, either radially (from the perinuclear region to the cell periphery) (7) or from side to side in a rectangular domain (86). In a disc-shaped system with randomly oriented filaments, the MFPT was found to depend largely on the total filament mass in the domain, with variability in arrival times increasing when the same mass is distributed into a few longer filaments (7). When passive states between processive runs were modeled as a subdiffusive continuous time random walk, the MFPT was found to decrease for long individual filaments (79). Such anomalous transport was also shown to yield a biphasic distribution of first passage times, with a bolus of particles arriving rapidly at the periphery followed by a long tail of slowly arriving particles, consistent with the behavior observed for glucose-stimulated delivery of insulin granules in pancreatic cells (134).

A key aspect of cytoskeletal architecture in a random network is the polarity distribution of the filaments. Reversing even a small fraction of outward-pointing filaments can substantially increase first passage times, and local 'traps' of converging polarity (Fig. 3a) contribute to configurations with unusually high MFPTs (7, 86). Junctions of three or more filaments with converging polarity give rise to vortex-like traps with power-law escape times that result in effectively glassy dynamics (107). The polarity of individual filaments was found to have a disproportionately high impact on the transit time when those filaments

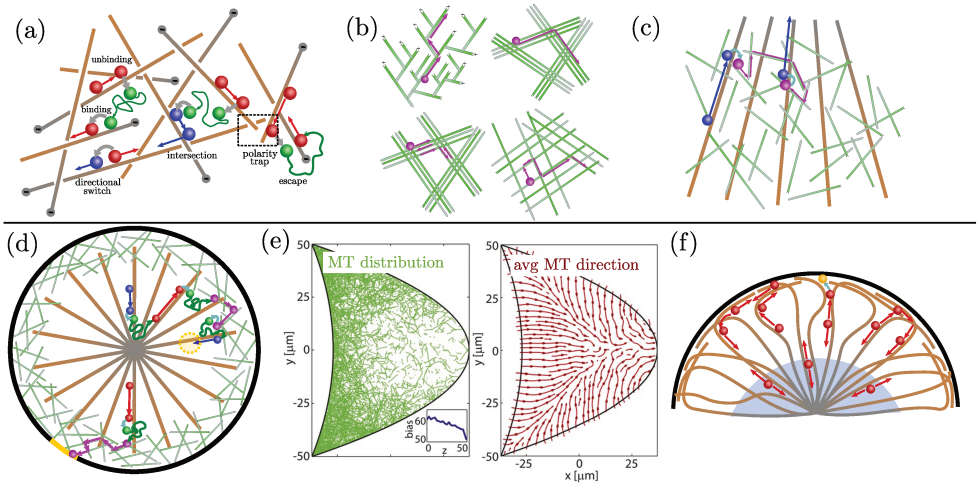

Figure 3

Transport modulation by density, polarity, and heterogeneous distribution of cytoskeletal networks. (a) Intermittent transport on an unpolarized, randomly oriented network of microtubules (brown). Cargo switches between a plus-end-directed state (red), a minus-end-directed state (blue) or a passive state (green). Localized polarity traps result in temporary accumulation of cargo. (b) Transport on actin structures is modulated by filament spacing and polarity. Globally polarized branched networks enable directed transport; polarity-aligned bundles yield long run-lengths; unpolarized structures with loose spacing enable more efficient diffusivity and reduced trapping compared to tightly-spaced bundles. (c) Interplay of transport along radially oriented microtubules and a randomly distributed actin network allows for regulated switching between perinuclear accumulation and broad dispersion. (d) Heterogeneous architectures with radial microtubules and a narrow peripheral actin network allow efficient cargo transport to targets on the cell surface and in the bulk (orange). (e) Simulated microtubule organization in stage 9 *Drosophila* oocyte, showing gradient in cortical nucleation density (left) and resulting average directionality of microtubules (right). Image adapted from Reference (128), CC BY. (f) High perinuclear microtubule density (blue region) enhances first passage times to periphery for bidirectionally moving cargo (red). Increased microtubule density near cortex may hinder accumulation of membrane-bound granules (orange) by enabling more rapid withdrawal of bidirectionally moving particles.

formed a unique forward path out of a localized trap region (86). The importance of cytoskeletal filament polarity and the formation of traps has also been observed experimentally for myosin-driven transport on reconstituted actin networks with a variety of branched and bundled architectures (76, 108) (Fig. 3b). These results imply that, in the absence of global filament polarization, different static architectures for the cytoskeletal network can result in highly variable transit times. Notably, dynamic turnover of the cytoskeletal filaments can rescue trapped cargo (61) and thus has the potential to both homogenize and speed up overall transport time.

In some systems, intermeshed cytoskeletal networks of actin and microtubule filaments can work together to control transport. Specifically, the distribution of pigment granules in *Xenopus* and fish oocytes undergoes regulated switching from dispersion to perinuclear convergence, in a manner dependent on the rate of transition between myosin-driven motion on a disorganized actin network and dynein-dominated transport along radially polarized

microtubule filaments (Fig. 3c) (94, 116, 118). In simulations, increasing the probability of actin to microtubule switching at each intersection is sufficient to trigger granule accumulation at the cell center, while reducing this rate allows granules to disperse broadly between periods of microtubule attachment (94, 118).

3.2.2. Spatially heterogeneous transport. An additional feature of motor-driven transport at the whole-cell scale is the spatial heterogeneity of cytoskeletal morphology. All of the previously discussed parameters of cytoskeletal architecture (density, polarity, filament length) can vary dramatically between different regions of the same cell, enabling further optimization of transport dynamics. In particular, a geometry with radially polarized microtubules in the perinuclear region coupled to randomly oriented short actin filaments at the cell periphery (Fig. 3d) is observed in many cell types. This arrangement enables cargos to perform long runs towards the surface, followed by an effective random walk along the peripheral layer. Modeling work indicates that such an architecture, together with biased anterograde movement on the radial microtubules, leads to optimal efficiency for finding narrow targets on the cell periphery (54, 112). To attain maximal rates of encounter with targets in the bulk of the cell, the optimal system was shown to have a similar heterogeneous geometry, with nearly unbiased direction of motion along the microtubules (112).

The microtubule cytoskeleton itself can exhibit heterogeneity across the cell, with densities depending on filament lengths and the arrangement of nucleation sites anchoring the minus ends. In mid-stage *Drosophila* oocytes, for instance, microtubules nucleate at the cell cortex with a gradient of decreasing density from the anterior to the posterior pole (95). This gradient gives rise to coupled steady-state patterns of cytoskeletal flows and microtubule orientation (Fig. 3e) that allow the posterior localization of kinesin and dynein-driven mRNAs to opposite poles of the oocyte (128). Interestingly, removing the bias in nucleation density leads to the formation of bifurcation points in the cytoskeletal pattern, such that cargo localization becomes dependent on its starting position.

For cargos with short processive runs, cellular regions with increased microtubule density correspond to areas of enhanced effective diffusivity (Fig. 3f). In a radially symmetric system, a band of heightened diffusivity placed near the nucleus has the greatest effect on speeding up first passage times to the cell periphery (7). In non-differentiated animal cell morphologies, increased microtubule density is indeed expected near the centrosome, a microtubule-organizing center located next to the nucleus (24).

Counterintuitively, increased microtubule density beneath the plasma membrane can actually hinder secretion of vesicle-encapsulated proteins by speeding up the withdrawal of particles from the periphery and interfering with anchoring interactions at the membrane. This effect has been observed for the peripheral accumulation of insulin granules in pancreatic β-cells, where microtubules can grow long enough to form a peripheral layer parallel to the membrane that reduces granule accumulation (20, 141) (Fig. 3f). Stimulation by glucose destabilizes microtubules, decreasing their typical length, reducing peripheral densities, and thereby enhancing insulin granule concentrations at the plasma membrane and promoting secretion.

4. Perspectives

Over the past several decades, the molecular-scale structure and mechanics of the components responsible for intracellular transport have been extensively characterized. The

load-dependence of molecular motors working individually (129) or in groups (55), as well as the myriads of regulatory biochemical modifications to motors, adaptors, and microtubules (11, 45, 92), have been explored both *in vitro* and *in vivo*. Similarly, the rheological properties of the cytoplasm (40, 53) and the dynamic behaviors of individual molecules (58, 68), vesicles (26, 130), and exogenous particles (40, 53, 69) have been well-quantified. With the advent of new super-resolution and correlative imaging methods, as well as 3D reconstruction techniques, the architecture and organization of subcellular components, including cytoskeletal networks (10, 130) and organelles (109, 131), have also been increasingly elucidated. Despite this plethora of structural and dynamic data, however, the inter-relationship of structure and function at the cellular scale remains a source of many open questions.

In this review, we have explored some of the many ways in which intracellular morphology can modulate transport dynamics, both for diffusing particles and for those undergoing motor-driven motion. A fundamentally important question for each of the example systems discussed is the extent to which the coupling between morphology and transport has an important impact on biological function. Is the networked morphology of structures such as the endoplasmic reticulum and mitochondria a critical aspect of their role as cellular transport and distribution networks for ions, metabolites, and secreted proteins? Is the distribution of branch widths or microtubule orientations in dendritic trees actively optimized to allow the efficient delivery of diffusing proteins or sorting of motor-driven vesicles?

These questions are beginning to be addressed by studies that focus on how transport dynamics are altered by experimental perturbations or existing natural variations in cell morphology. Such measurements have indicated, for instance, that narrowing of ER tubules reduces luminal protein spreading (66), and that activation of a cyclic-AMP signaling pathway in narrower dendritic branches allows longer-range transport of the signal towards the nucleus (70). A variety of perturbations to cellular architecture and ER morphology are also associated with neurodegenerative diseases such as Alzheimer's disease (117) and hereditary spastic paraplegia (28), whose mechanistic basis is thought to involve defects in axonal transport (84).

Unraveling the functional effects of transport alterations arising from perturbed intracellular morphology requires a detailed understanding of the specific objective fulfilled by each transport process. For example, the efficiency of sorting, dispersion, or distal delivery will be affected differently by alterations in cytoskeletal filament polarity. Because the same cytoskeletal highways support the movement of a broad variety of particles with different transport needs, we would expect each of these objectives to play a role in cellular processes. Similarly, morphological changes that enhance the accumulation of membrane-bound proteins in specialized cell regions (*eg:* photoreceptor outer segments) may simultaneously hinder the diffusion-limited interaction kinetics of aqueous proteins that must maneuver around expanded membranous obstructions. The same tubular networks that enable rapid delivery of proteins throughout the cell bulk must also serve as obstacles for the diffusive and motor-driven transport of cytoplasmic vesicles that maneuver around the tubules.

It is thus critical to explore the full broad diversity of questions regarding how individual cellular structures modulate different transport objectives, be they speed of delivery or precision of distribution. Developing a comprehensive picture of the coupling between morphology and transport is a crucial step on the path leading from static imaging of intracellular architecture to a quantitatively predictive understanding of functional consequences arising from morphological perturbations.

DISCLOSURE STATEMENT

The authors are not aware of any affiliations, memberships, funding, or financial holdings that might be perceived as affecting the objectivity of this review.

ACKNOWLEDGMENTS

This work was supported by National Science Foundation (NSF) CAREER grant #1848057 to EFK, NSF grant #2034482 to EFK, and a Cottrell Scholar Award to EFK from the Research Corporation for Science Advancement.

LITERATURE CITED

1. Abel SM, Roose JP, Groves JT, Weiss A, Chakraborty AK. 2012. The membrane environment can promote or suppress bistability in cell signaling networks. *J Phys Chem B* 116(11):3630–3640
2. Agrawal A, Koslover EF. 2021. Optimizing mitochondrial maintenance in extended neuronal projections. *Plos Comput Biol* 17(6):e1009073
3. Agrawal A, Pekkurnaz G, Koslover EF. 2018. Spatial control of neuronal metabolism through glucose-mediated mitochondrial transport regulation. *elife* 7:e40986
4. Alim K. 2018. Fluid flows shaping organism morphology. *Philosophical Transactions of the Royal Society B: Biological Sciences* 373(1747):20170112
5. Alim K, Amselem G, Peaudecerf F, Brenner MP, Pringle A. 2013. Random network peristalsis in physarum polycephalum organizes fluid flows across an individual. *P Natl Acad Sci* 110(33):13306–13311
6. Alim K, Andrew N, Pringle A, Brenner MP. 2017. Mechanism of signal propagation in physarum polycephalum. *P Natl Acad Sci* 114(20):5136–5141
7. Ando D, Korabel N, Huang KC, Gopinathan A. 2015. Cytoskeletal network morphology regulates intracellular transport dynamics. *Biophys J* 109(8):1574–1582
8. Aon MA, Cortassa S. 2015. Function of metabolic and organelle networks in crowded and organized media. *Front Physiol* 5:523
9. Aris R. 1956. On the dispersion of a solute in a fluid flowing through a tube. *P Roy Soc A-Math Phy* 235(1200):67–77
10. Bálint Š, Verdeny Vilanova I, Sandoval Álvarez Á, Lakadamyali M, Vilanova IV, et al. 2013. Correlative live-cell and superresolution microscopy reveals cargo transport dynamics at microtubule intersections. *Proc. Natl. Acad. Sci.* 110(9):3375–3380
11. Barlan K, Gelfand VI. 2017. Microtubule-based transport and the distribution, tethering, and organization of organelles. *Cold Spring Harbor perspectives in biology* 9(5):a025817
12. Barlan K, Lu W, Gelfand VI. 2013. The microtubule-binding protein ensconsin is an essential cofactor of kinesin-1. *Curr Biol* 23(4):317–322
13. Barthélemy M. 2011. Spatial networks. *Physics Reports* 499(1-3):1–101
14. Bassingthwaighte JB, Liebovitch LS, West BJ. 2013. *Fractal physiology*. Springer
15. Baum M, Erdel F, Wachsmuth M, Rippe K. 2014. Retrieving the intracellular topology from multi-scale protein mobility mapping in living cells. *Nat Commun* 5(1):1–12
16. Ben-Avraham D, Havlin S. 2000. *Diffusion and reactions in fractals and disordered systems*. Cambridge university press
17. Bénichou O, Chevalier C, Klafter J, Meyer B, Voituriez R. 2010. Geometry-controlled kinetics. *Nat Chem* 2(6):472
18. Bénichou O, Voituriez R. 2008. Narrow-escape time problem: time needed for a particle to exit a confining domain through a small window. *Phys Rev Lett* 100(16):168105

19. Boergens KM, Kapfer C, Helmstaedter M, Denk W, Borst A. 2018. Full reconstruction of large lobula plate tangential cells in drosophila from a 3d em dataset. *PloS one* 13(11):e0207828
20. Bracey KM, Ho KH, Yampolsky D, Gu G, Kaverina I, Holmes WR. 2020. Microtubules regulate localization and availability of insulin granules in pancreatic beta cells. *Biophys J* 118(1):193–206
21. Bressloff PC, Newby JM. 2013. Stochastic models of intracellular transport. *Rev. Mod. Phys.* 85(1):135–196
22. Brown AI, Koslover EF. 2019. Drive, filter, and stick: A protein sorting conspiracy in photoreceptors. *J Cell Biol* 218(11):3533–3534
23. Brown AI, Westrate LM, Koslover EF. 2020. Impact of global structure on diffusive exploration of organelle networks. *Sci Rep* 10(1):1–13
24. Burute M, Kapitein LC. 2019. Cellular logistics: unraveling the interplay between microtubule organization and intracellular transport. *Annu Rev Cell Dev Bi* 35:29–54
25. Calvert PD, Schiesser WE, Pugh EN. 2010. Diffusion of a soluble protein, photoactivatable gfp, through a sensory cilium. *J Gen Physiol* 135(3):173–196
26. Chen K, Wang B, Granick S. 2015. Memoryless self-reinforcing directionality in endosomal active transport within living cells. *Nat Mater* 14(6):589–593
27. Chiu SY. 2011. Matching mitochondria to metabolic needs at nodes of ranvier. *Neuroscientist* 17(4):343–350
28. Chiurchiu V, Maccarrone M, Orlacchio A. 2014. The role of reticulons in neurodegenerative diseases. *Neuromol Med* 16(1):3–15
29. Chubynsky MV, Slater GW. 2014. Diffusing diffusivity: a model for anomalous, yet brownian, diffusion. *Phys Rev Lett* 113(9):098302
30. Condamin S, Bénichou O, Tejedor V, Voituriez R, Klafter J. 2007. First-passage times in complex scale-invariant media. *Nature* 450(7166):77–80
31. de la Rosa MAD, Koslover EF, Mulligan PJ, Spakowitz AJ. 2010. Dynamic strategies for target-site search by dna-binding proteins. *Biophys J* 98(12):2943–2953
32. Dieteren CE, Gielen SC, Nijtmans LG, Smeitink JA, Swarts HG, et al. 2011. Solute diffusion is hindered in the mitochondrial matrix. *P Natl Acad Sci* 108(21):8657–8662
33. Dix JA, Verkman A. 2008. Crowding effects on diffusion in solutions and cells. *Annu. Rev. Biophys.* 37:247–263
34. Dixit R, Ross JL, Goldman YE, Holzbaur EL. 2008. Differential regulation of dynein and kinesin motor proteins by tau. *Science* 319(5866):1086–1089
35. Dora M, Holcman D. 2020. Active flow network generates molecular transport by packets: case of the endoplasmic reticulum. *Proceedings of the Royal Society B* 287(1930):20200493
36. Doyle M, Kiebler MA. 2011. Mechanisms of dendritic mrna transport and its role in synaptic tagging. *Embo J* 30(17):3540–3552
37. Farías GG, Guardia CM, Britt DJ, Guo X, Bonifacino JS. 2015. Sorting of dendritic and axonal vesicles at the pre-axonal exclusion zone. *Cell Rep* 13(6):1221–1232
38. Ferrante M, Migliore M, Ascoli GA. 2013. Functional impact of dendritic branch-point morphology. *J Neurosci* 33(5):2156–2165
39. Ferree AW, Trudeau K, Zik E, Benador IY, Twig G, et al. 2013. Mitotimer probe reveals the impact of autophagy, fusion, and motility on subcellular distribution of young and old mitochondrial protein and on relative mitochondrial protein age. *Autophagy* 9(11):1887–1896
40. Fodor É, Guo M, Gov N, Visco P, Weitz D, van Wijland F. 2015. Activity-driven fluctuations in living cells. *Europhys Lett* 110(4):48005
41. Fonkeu Y, Kraynyukova N, Hafner AS, Kochen L, Sartori F, et al. 2019. How mrna localization and protein synthesis sites influence dendritic protein distribution and dynamics. *Neuron* 103(6):1109–1122
42. Frey T, Renken C, Perkins G. 2002. Insight into mitochondrial structure and function from electron tomography. *Bba-bioenergetics* 1555(1-3):196–203

43. Fricker MD, Heaton LL, Jones NS, Boddy L. 2017. The mycelium as a network. *Microbiology spectrum* 5(3)
44. Friedman JR, Voeltz GK. 2011. The er in 3d: a multifunctional dynamic membrane network. *Trends Cell Biol* 21(12):709–717
45. Fu Mm, Holzbaur EL. 2014. Integrated regulation of motor-driven organelle transport by scaffolding proteins. *Trends Cell Biol* 24(10):564–574
46. Gagnon JA, Mowry KL. 2011. Molecular motors: directing traffic during rna localization. *Crit Rev Biochem Mol* 46(3):229–239
47. Gastner MT, Newman ME. 2006. The spatial structure of networks. *Eur Phys J B* 49(2):247–252
48. Glock C, Heumüller M, Schuman EM. 2017. mrna transport & local translation in neurons. *Curr Opin Neurobiol* 45:169–177
49. Godec A, Metzler R. 2015. Signal focusing through active transport. *Phys Rev E* 92(1):010701
50. Goldstein RE, van de Meent JW. 2015. A physical perspective on cytoplasmic streaming. *Interface focus* 5(4):20150030
51. Grebenkov DS, Tupikina L. 2018. Heterogeneous continuous-time random walks. *Phys Rev E* 97(1):012148
52. Guedes-Dias P, Nirschl JJ, Abreu N, Tokito MK, Janke C, et al. 2019. Kinesin-3 responds to local microtubule dynamics to target synaptic cargo delivery to the presynapse. *Curr Biol* 29(2):268–282
53. Guo M, Ehrlicher AJ, Jensen MH, Renz M, Moore JR, et al. 2014. Probing the stochastic, motor-driven properties of the cytoplasm using force spectrum microscopy. *Cell* 158(4):822–832
54. Hafner AE, Rieger H. 2018. Spatial cytoskeleton organization supports targeted intracellular transport. *Biophys J* 114(6):1420–1432
55. Hancock WO. 2014. Bidirectional cargo transport: moving beyond tug of war. *Nat Rev Mol Cell Biol* 15(9):615
56. Harris JJ, Jolivet R, Attwell D. 2012. Synaptic energy use and supply. *Neuron* 75(5):762–777
57. Hirokawa N, Noda Y, Tanaka Y, Niwa S. 2009. Kinesin superfamily motor proteins and intracellular transport. *Nat Rev Mol Cell Bio* 10(10):682–696
58. Holcman D, Parutto P, Chambers JE, Fantham M, Young LJ, et al. 2018. Single particle trajectories reveal active endoplasmic reticulum luminal flow. *Nat Cell Biol* 20(10):1118
59. Huber G, Wilkinson M. 2019. Terasaki spiral ramps and intracellular diffusion. *Phys Biol* 16(6):065002
60. Jose R, Santen L, Shaebani MR. 2018. Trapping in and escape from branched structures of neuronal dendrites. *Biophys J* 115(10):2014–2025
61. Jung W, Tabatabai AP, Thomas JJ, Tabei SA, Murrell MP, Kim T. 2019. Dynamic motions of molecular motors in the actin cytoskeleton. *Cytoskeleton* 76(11-12):517–531
62. Kapitein LC, Hoogenraad CC. 2011. Which way to go? cytoskeletal organization and polarized transport in neurons. *Mol Cell Neurosci* 46(1):9–20
63. Kapitein LC, Hoogenraad CC. 2015. Building the neuronal microtubule cytoskeleton. *Neuron* 87(3):492–506
64. Kapitein LC, Schlager MA, Kuijpers M, Wulf PS, van Spronsen M, et al. 2010. Mixed microtubules steer dynein-driven cargo transport into dendrites. *Curr Biol* 20(4):290–299
65. Klafter J, Lim S, Metzler R. 2012. Fractional dynamics: recent advances
66. Konno T, Parutto P, Bailey DM, Davì V, Crapart C, et al. 2021. Endoplasmic reticulum morphological regulation by rtn4/nogo modulates neuronal regeneration by slowing luminal transport. *bioRxiv*
67. Kühn T, Ihalainen TO, Hyväluoma J, Dross N, Willman SF, et al. 2011. Protein diffusion in mammalian cell cytoplasm. *PloS one* 6(8):e22962
68. Lampo TJ, Stylianidou S, Backlund MP, Wiggins PA, Spakowitz AJ. 2017. Cytoplasmic rna-

protein particles exhibit non-gaussian subdiffusive behavior. *Biophys J* 112(3):532–542
69. Li H, Dou SX, Liu YR, Li W, Xie P, et al. 2015. Mapping intracellular diffusion distribution using single quantum dot tracking: compartmentalized diffusion defined by endoplasmic reticulum. *J Am Chem Soc* 137(1):436–444
70. Li L, Gervasi N, Girault JA. 2015. Dendritic geometry shapes neuronal camp signalling to the nucleus. *Nat Commun* 6(1):1–15
71. Li R, Fowler JA, Todd BA. 2014. Calculated rates of diffusion-limited reactions in a three-dimensional network of connected compartments: application to porous catalysts and biological systems. *Phys Rev Lett* 113(2):028303
72. Liao M, Howard J. 2020. The narrowing of dendrite branches across nodes follows a well-defined scaling law. *bioRxiv*
73. Lin C, Zhang Y, Sparkes I, Ashwin P. 2014. Structure and dynamics of er: minimal networks and biophysical constraints. *Biophys J* 107(3):763–772
74. Lizana L, Konkoli Z. 2005. Diffusive transport in networks built of containers and tubes. *Phys Rev E* 72(2):026305
75. Lizana L, Konkoli Z, Bauer B, Jesorka A, Orwar O. 2009. Controlling chemistry by geometry in nanoscale systems. *Annu Rev Phys Chem* 60:449–468
76. Lombardo AT, Nelson SR, Kennedy GG, Trybus KM, Walcott S, Warshaw DM. 2019. Myosin va transport of liposomes in three-dimensional actin networks is modulated by actin filament density, position, and polarity. *P Natl Acad Sci* 116(17):8326–8335
77. Maday S, Twelvetrees AE, Moughamian AJ, Holzbaur EL. 2014. Axonal transport: cargo-specific mechanisms of motility and regulation. *Neuron* 84(2):292–309
78. Maday S, Wallace KE, Holzbaur EL. 2012. Autophagosomes initiate distally and mature during transport toward the cell soma in primary neurons. *J Cell Biol* 196(4):407–417
79. Maelfeyt B, Tabei SA, Gopinathan A. 2019. Anomalous intracellular transport phases depend on cytoskeletal network features. *Phys Rev E* 99(6):062404
80. Marbach S, Alim K, Andrew N, Pringle A, Brenner MP. 2016. Pruning to increase taylor dispersion in physarum polycephalum networks. *Phys Rev Lett* 117(17):178103
81. Masuda N, Porter MA, Lambiotte R. 2017. Random walks and diffusion on networks. *Physics reports* 716:1–58
82. Maza NA, Schiesser WE, Calvert PD. 2019. An intrinsic compartmentalization code for peripheral membrane proteins in photoreceptor neurons. *J Cell Biol* 218(11):3753–3772
83. Meigel FJ, Alim K. 2018. Flow rate of transport network controls uniform metabolite supply to tissue. *J Roy Soc Interface* 15(142):20180075
84. Millecamps S, Julien JP. 2013. Axonal transport deficits and neurodegenerative diseases. *Nat Rev Neurosci* 14(3):161–176
85. Milo R, Phillips R. 2015. *Cell biology by the numbers*. Garland Science
86. Mlynarczyk PJ, Abel SM. 2019. First passage of molecular motors on networks of cytoskeletal filaments. *Phys Rev E* 99(2):022406
87. Mogre S, Christensen JR, Reck-Peterson SL, Koslover EF. 2021. Optimizing microtubule arrangements for rapid cargo capture. *bioRxiv*
88. Mogre SS, Brown AI, Koslover EF. 2020. Getting around the cell: physical transport in the intracellular world. *Phys Biol* 17(6):061003
89. Mogre SS, Christensen JR, Niman CS, Reck-Peterson SL, Koslover EF. 2020. Hitching a ride: Mechanics of transport initiation through linker-mediated hitchhiking. *Biophys J* 118(6):1357–1369
90. Moughamian AJ, Osborn GE, Lazarus JE, Maday S, Holzbaur EL. 2013. Ordered recruitment of dynactin to the microtubule plus-end is required for efficient initiation of retrograde axonal transport. *J Neurosci* 33(32):13190–13203
91. Najafi M, Maza NA, Calvert PD. 2012. Steric volume exclusion sets soluble protein concentrations in photoreceptor sensory cilia. *P Natl Acad Sci* 109(1):203–208

92. Nirschl JJ, Ghiretti AE, Holzbaur EL. 2017. The impact of cytoskeletal organization on the local regulation of neuronal transport. *Nat Rev Neurosci* 18(10):585–597
93. Noh JD, Rieger H. 2004. Random walks on complex networks. *Phys Rev Lett* 92(11):118701
94. Oberhofer A, Reithmann E, Spieler P, Stepp WL, Zimmermann D, et al. 2020. Molecular underpinnings of cytoskeletal cross-talk. *P Natl Acad Sci* 117(8):3944–3952
95. Parton RM, Hamilton RS, Ball G, Yang L, Cullen CF, et al. 2011. A par-1–dependent orientation gradient of dynamic microtubules directs posterior cargo transport in the drosophila oocyte. *J Cell Biol* 194(1):121–135
96. Pekkurnaz G, Trinidad JC, Wang X, Kong D, Schwarz TL. 2014. Glucose regulates mitochondrial motility via milton modification by o-glcnac transferase. *Cell* 158(1):54–68
97. Quinlan ME. 2016. Cytoplasmic streaming in the drosophila oocyte. *Annu Rev Cell Dev Bi* 32:173–195
98. Rangaraju V, Calloway N, Ryan TA. 2014. Activity-driven local atp synthesis is required for synaptic function. *Cell* 156(4):825–835
99. Rangaraju V, Lauterbach M, Schuman EM. 2019. Spatially stable mitochondrial compartments fuel local translation during plasticity. *Cell* 176(1-2):73–84
100. Reck-Peterson SL, Redwine WB, Vale RD, Carter AP. 2018. The cytoplasmic dynein transport machinery and its many cargoes. *Nat Rev Mol Cell Bio* 19(6):382
101. Ronellenfitsch H, Katifori E. 2016. Global optimization, local adaptation, and the role of growth in distribution networks. *Phys Rev Lett* 117(13):138301
102. Sadegh S, Higgins JL, Mannion PC, Tamkun MM, Krapf D. 2017. Plasma membrane is compartmentalized by a self-similar cortical actin meshwork. *Phys Rev X* 7(1):011031
103. Sallee MD, Feldman JL. 2021. Microtubule organization across cell types and states. *Curr Biol* 31(10):R506–R511
104. Salogiannis J, Reck-Peterson SL. 2017. Hitchhiking: a non-canonical mode of microtubule-based transport. *Trends Cell Biol* 27(2):141–150
105. Santamaria F, Wils S, De Schutter E, Augustine GJ. 2006. Anomalous diffusion in purkinje cell dendrites caused by spines. *Neuron* 52(4):635–648
106. Sartori F, Hafner AS, Karimi A, Nold A, Fonkeu Y, et al. 2020. Statistical laws of protein motion in neuronal dendritic trees. *Cell Rep* 33(7):108391
107. Scholz M, Burov S, Weirich KL, Scholz BJ, Tabei SA, et al. 2016. Cycling state that can lead to glassy dynamics in intracellular transport. *Phys Rev X* 6(1):011037
108. Scholz M, Weirich KL, Gardel ML, Dinner AR. 2020. Tuning molecular motor transport through cytoskeletal filament network organization. *Soft Matter* 16(8):2135–2140
109. Schroeder LK, Barentine AE, Merta H, Schweighofer S, Zhang Y, et al. 2019. Dynamic nanoscale morphology of the er surveyed by sted microscopy. *J Cell Biol* 218(1):83–96
110. Schuss Z, Singer A, Holcman D. 2007. The narrow escape problem for diffusion in cellular microdomains. *P Natl Acad Sci* 104(41):16098–16103
111. Schuster M, Kilaru S, Ashwin P, Lin C, Severs NJ, Steinberg G. 2011. Controlled and stochastic retention concentrates dynein at microtubule ends to keep endosomes on track. *Embo J* 30(4):652–664
112. Schwarz K, Schröder Y, Qu B, Hoth M, Rieger H. 2016. Optimality of spatially inhomogeneous search strategies. *Phys Rev Lett* 117(6):068101
113. Schwarz TL. 2013. Mitochondrial trafficking in neurons. *Cold Spring Harbor perspectives in biology* 5(6):a011304
114. Scott ZC, Brown AI, Mogre SS, Westrate LM, Koslover EF. 2021. Diffusive search and trajectories on spatial networks: a propagator approach. *arXiv preprint arXiv:2103.05065*
115. Shen L, Chen Z. 2007. Critical review of the impact of tortuosity on diffusion. *Chem Eng Sci* 62(14):3748–3755
116. Slepchenko BM, Semenova I, Zaliapin I, Rodionov V. 2007. Switching of membrane organelles between cytoskeletal transport systems is determined by regulation of the microtubule-based

transport. *J Cell Biol* 179(4):635–641
117. Smith DL, Pozueta J, Gong B, Arancio O, Shelanski M. 2009. Reversal of long-term dendritic spine alterations in alzheimer disease models. *P Natl Acad Sci* 106(39):16877–16882
118. Snider J, Lin F, Zahedi N, Rodionov V, Clare CY, Gross SP. 2004. Intracellular actin-based transport: how far you go depends on how often you switch. *P Natl Acad Sci* 101(36):13204–13209
119. Song Ah, Wang D, Chen G, Li Y, Luo J, et al. 2009. A selective filter for cytoplasmic transport at the axon initial segment. *Cell* 136(6):1148–1160
120. Stauffer D, Aharony A. 1994. *Introduction to percolation theory*. CRC Press
121. Stepanek L, Pigino G. 2016. Microtubule doublets are double-track railways for intraflagellar transport trains. *Science* 352(6286):721–724
122. Sukhorukov VM, Dikov D, Reichert AS, Meyer-Hermann M. 2012. Emergence of the mitochondrial reticulum from fission and fusion dynamics. *PLoS Comput Biol* 8(10):e1002745
123. Takahashi K, Tănase-Nicola S, Ten Wolde PR. 2010. Spatio-temporal correlations can drastically change the response of a mapk pathway. *P Natl Acad Sci* 107(6):2473–2478
124. Tas RP, Chazeau A, Cloin BM, Lambers ML, Hoogenraad CC, Kapitein LC. 2017. Differentiation between oppositely oriented microtubules controls polarized neuronal transport. *Neuron* 96(6):1264–1271
125. Taschner M, Lorentzen E. 2016. The intraflagellar transport machinery. *Cold Spring Harbor perspectives in biology* 8(10):a028092
126. Terasaki M, Shemesh T, Kasthuri N, Klemm RW, Schalek R, et al. 2013. Stacked endoplasmic reticulum sheets are connected by helicoidal membrane motifs. *Cell* 154(2):285–296
127. Tønnesen J, Nägerl UV. 2016. Dendritic spines as tunable regulators of synaptic signals. *Frontiers in psychiatry* 7:101
128. Trong PK, Doerflinger H, Dunkel J, St Johnston D, Goldstein RE. 2015. Cortical microtubule nucleation can organise the cytoskeleton of drosophila oocytes to define the anteroposterior axis. *elife* 4:e06088
129. Vale RD. 2003. The Molecular Motor Toolbox for Intracellular Transport. *Cell* 112(4):467–480
130. Verdeny-Vilanova I, Wehnekamp F, Mohan N, Álvarez ÁS, Borbely JS, et al. 2017. 3d motion of vesicles along microtubules helps them to circumvent obstacles in cells. *J Cell Sci* 130(11):1904–1916
131. Viana MP, Brown AI, Mueller IA, Goul C, Koslover EF, Rafelski SM. 2020. Mitochondrial Fission and Fusion Dynamics Generate Efficient, Robust, and Evenly Distributed Network Topologies in Budding Yeast Cells. *Cell Syst* 10(3):287–297.e5
132. Volland S, Hughes LC, Kong C, Burgess BL, Linberg KA, et al. 2015. Three-dimensional organization of nascent rod outer segment disk membranes. *P Natl Acad Sci* 112(48):14870–14875
133. Wang B, Kuo J, Bae SC, Granick S. 2012. When brownian diffusion is not gaussian. *Nat Mater* 11(6):481
134. Wang Z, Thurmond DC. 2009. Mechanisms of biphasic insulin-granule exocytosis–roles of the cytoskeleton, small gtpases and snare proteins. *J Cell Sci* 122(7):893–903
135. Westrate L, Lee J, Prinz W, Voeltz G. 2015. Form follows function: the importance of endoplasmic reticulum shape. *Annu Rev Biochem* 84:791–811
136. Williams AH, O'donnell C, Sejnowski TJ, O'leary T. 2016. Dendritic trafficking faces physiologically critical speed-precision tradeoffs. *elife* 5:e20556
137. Wong MY, Zhou C, Shakiryanova D, Lloyd TE, Deitcher DL, Levitan ES. 2012. Neuropeptide delivery to synapses by long-range vesicle circulation and sporadic capture. *Cell* 148(5):1029–1038
138. Yau KW, Schätzle P, Tortosa E, Pagès S, Holtmaat A, et al. 2016. Dendrites in vitro and in vivo contain microtubules of opposite polarity and axon formation correlates with uniform plus-end-out microtubule orientation. *J Neurosci* 36(4):1071–1085

139. Yogev S, Cooper R, Fetter R, Horowitz M, Shen K. 2016. Microtubule organization determines axonal transport dynamics. *Neuron* 92(2):449–460
140. Zamponi N, Zamponi E, Cannas SA, Billoni OV, Helguera PR, Chialvo DR. 2018. Mitochondrial network complexity emerges from fission/fusion dynamics. *Sci Rep* 8(1):1–10
141. Zhu X, Hu R, Brissova M, Stein RW, Powers AC, et al. 2015. Microtubules negatively regulate insulin secretion in pancreatic β cells. *Dev Cell* 34(6):656–668
142. Zwanzig R. 1992. Diffusion past an entropy barrier. *J Phys Chem-us* 96(10):3926–3930